

Adapting Dual-encoder Vision-language Models for Paraphrased Retrieval

Jiacheng Cheng^{1*}, Hijung Valentina Shin², Nuno Vasconcelos¹, Bryan Russell², Fabian Caba Heilbron²
¹UC San Diego ²Adobe Research



Figure 1. **Paraphrased retrieval.** **1(a):** The CLIP model [48] often returns very different top retrievals for two text queries that are paraphrases of each other. In this example, the paraphrased query differs by a single word: “*kid*”→“*child*”. **1(b):** Our approach returns similar top retrievals for paraphrased queries by adapting a frozen pretrained language model during dual encoder training. We outline images in green that appear in the top retrievals for the original and paraphrased queries.

Abstract

In the recent years, the dual-encoder vision-language models (e.g. CLIP) have achieved remarkable text-to-image retrieval performance. However, we discover that these models usually results in very different retrievals for a pair of paraphrased queries. Such behavior might render the retrieval system less predictable and lead to user frustration. In this work, we consider the task of paraphrased text-to-image retrieval where a model aims to return similar results given a pair of paraphrased queries. To start with, we collect a dataset of paraphrased image descriptions to facilitate quantitative evaluation for this task. We then hypothesize that the undesired behavior of existing dual-encoder model is due to their text towers which are trained on image-sentence pairs and lack the ability to capture the semantic similarity between paraphrased queries. To improve on this, we investigate multiple strategies for training a dual-encoder model starting from a language model pretrained on a large text corpus. Compared to public dual-encoder models such as CLIP and OpenCLIP, the model trained with our best adaptation strategy achieves a significantly higher ranking similarity for paraphrased queries while maintaining similar zero-shot classification and retrieval accuracy.

1. Introduction

The dual-encoder vision-language foundation models (VLFMs) such as CLIP [48] have demonstrated promising zero-shot accuracy in text-image retrieval. However, in practice, their returned top retrievals are often very different for paraphrased queries. Consider the input text queries and the output visual search results produced by CLIP in Figure 1(a). In this example, when a single word is changed in the query (“*kid*”→“*child*”), even though the semantic meaning of the query remains almost exactly the same, all but one of the images returned by CLIP are completely different. If small changes in the user prompt lead to very different output, the results can be interpreted as unpredictable. Consequently, the construction of appropriate queries can be challenging and lead to a negative user experience when the model is used in downstream search applications.

We conjecture that these results are caused by the training of the CLIP model starting from random initialization on a limited text dataset of 400M sentences (paired with images). This text dataset has the following shortcomings that impair effective learning of paraphrases. First, it is significantly smaller than datasets used for training large language models. Recent large language models are trained

*Work partially done during an internship at Adobe Research.

on datasets that are orders of magnitude larger [8], allowing for greater exposure to paraphrase examples. Second, the sentences are consumed in isolation and not in the context of other sentences and paragraphs. This latter context is essential for long-range reasoning in learning to paraphrase. Third, the alt texts used for training CLIP are often noisy and not even complete sentences [17, 21, 54], which may hinder paraphrase learning.

Large language models pretrained on large text corpora have largely addressed these limitations. Moreover, these models have demonstrated impressive results on a variety of downstream language understanding tasks, including sentence semantic similarity [10] and paraphrase detection [19]. There have been prior efforts attempting to guide vision-language model training with pretrained language models [3, 37, 61]. However, most of them are successful for fusion-encoder models (*e.g.* BLIP-2 [37], Flamingo [3]). LiT [64] proposed to adopt a frozen supervised pretrained model in the image tower and training from scratch or finetuning the text tower for best zero-shot classification accuracy. When they plugged in a frozen pretrained language model into the dual-encoder architecture, they showed a significant degradation in the zero-shot accuracy of the resulting model. Unfreezing and finetuning the pretrained text tower can improve the zero-shot retrieval/classification accuracy. However, as we will demonstrate in the experiments, this strategy suffers from vastly different retrieval results for paraphrased language queries. In this paper, we seek to address this key question: can we train a dual-encoder vision-language model guided by a strong language model pretrained on a large text corpora? An ideal model will maintain the prior zero-shot retrieval/classification accuracy while better handling paraphrased language queries.

In this work, we show how to overcome the above limitations by guiding dual-encoder VLFMs training with pretrained language models. As our first contribution, we show that adding a set of alignment layers in the language tower significantly improves the zero-shot classification and retrieval accuracy compared to LiT’s locked language tower setting [64]. As our second contribution, we collect a dataset of paraphrased sentences paired with natural images for evaluating whether paraphrased language queries result in different retrievals. We compute the rank similarity of paraphrased language queries and, as our final contribution, show empirically that our adaptation strategy results in a significant improvement, as illustrated in Figure 1(b).

The rest of this paper is structured as follows. The related work is discussed in Sec. 2. In Sec. 3, we introduce our collected dataset and evaluation metrics for quantitatively measuring the rank similarity in paraphrased text-image retrieval. Aiming to improve the rank similarity in paraphrased retrieval, we present multiple strategies for training dual-encoder models starting from a pretrained lan-

guage model in Sec. 4 and comprehensively compare them in Sec. 5. In Sec. 6, we conclude our paper.

2. Related Work

Information Retrieval. *Synonymy* refers to the problem that different query terms with same or similar meaning cannot be properly handled by a information retrieval system and finally lead to undesired outcomes (*e.g.* low recall, user frustration). It is a well-known issue and has been extensively studied in the information retrieval literature [5, 40]. To address it, many techniques have been proposed. Latent semantic indexing (LSI) [15, 34] is able to discover relationships between words/terms in documents and thus reduce the effects of synonyms. However, the application of LSI for a dynamic corpus is prohibitive since it does not support ad-hoc addition of new documents [23]. Two popular alternative techniques are relevance feedback [52, 53] and query expansion (QE) [4, 9]. Relevance feedback refines the search results according to the users’ feedback on the initial search results, making it impractical when users are not involved in the retrieval process. QE expands the original query by adding semantically similar words from a pre-built thesaurus (*e.g.* WordNet [41, 42]). The performance of QE is usually sensitive to the quality of the word sense disambiguation in the query. In this work, we show that QE alone is not an effective solution to increase ranking similarity in paraphrased retrieval.

Vision-Language Foundation Models (VLFMs). There are two mainstream categories for VLFMs: (1) Dual-encoder models which have two separate image and text encoders [31, 48, 62, 64]. Dual-encoder models are usually pretrained by contrastive image-text learning and shown to be a strong zero-shot learner on many downstream cross-modal tasks (*e.g.*, image classification and image/text retrieval). (2) Fusion-encoder models with additional cross-modal encoders [12, 35–37, 58, 65]. In general, fusion-encoder models are pretrained with a combination of unimodal, multi-modal, cross-modal objectives. Although fusion-encoder models are superior in many vision-language tasks, they are usually significantly less efficient than dual-encoder models for large-scale image/text retrieval. In light of this, we focus on dual-encoder models for paraphrased retrieval in this work.

Robustness to Text Perturbations. According to a recent investigation [46], the retrieval performance of many vision-language models including CLIP is sensitive to many text perturbations such as synonym replacement and word swap. Although these text perturbations may not be equivalent to paraphrasing, they are widely existing in real-world scenarios. In the experiment section, our proposed training strategy is evaluated on different text perturbations and shown to achieve higher robustness.

3. Paraphrased Text-Image Retrieval

In order to perform quantitative evaluation of different vision-language models in paraphrased text-image retrieval, it is necessary to establish a dataset consisting of semantically equivalent natural language queries (paraphrase pairs) paired with corresponding images. We build on the MS COCO Captions multimodal dataset [38], which features a large quantity of images with high-quality captions. We used the captions of its 5K validation images as source data for collecting paraphrase pairs. Finally, 4155 paraphrase pairs are collected by automatic paraphrase generation and manual verification. To simulate image databases at different scales, we construct two image galleries. The smaller one consists of 5K images in the COCO validation set. The larger one is formulated by the combination of 5K validation and 123K unlabeled images in COCO. These two settings are denoted as COCO Paraphrased retrieval and COCO Paraphrased retrieval Extended (shorted as COCO-P and COCO-PE in the following) respectively. We describe next how we collect the paraphrased sentences and how we measure the rank similarity between the retrieval results for a query sentence and its paraphrase.

Paraphrase Collection. It is expensive and time consuming to generate high-quality sentence-level paraphrases at a large scale by human annotators. Consequently, traditional paraphrase datasets (e.g., Microsoft Research Paraphrase Corpus [19], Quora Question Pairs [1]) are constructed by first mining from newspapers/web sites followed by manual verification by a human. However, such approach does not serve our need since it is inefficient or even infeasible to find sentences with the equivalent meaning as certain image captions by web mining.

An alternative approach is to generate paraphrase candidates for captions automatically. Automatic paraphrase generation is a longstanding and challenging task in natural language processing [66]. Fortunately, the success of large autoregressive language models with billions of parameters (e.g., GPT-2/3 [8, 47]) renders it possible to generate automatically high-quality paraphrase candidates in an unsupervised or few-shot manner [27, 59, 60].

Inspired by these successful applications, we adopted GPT-3 for paraphrasing image captions. We chose 5000 captions describing the images in the validation set of the MS COCO Captions dataset as the source data. For each original caption, we generated 5 paraphrase candidates via 5 independent runs of GPT-3 with manually chosen hyperparameters and prompts (see supplemental material). We show some examples in Fig. 2. In practice, we observe that most of the paraphrase candidates are of decent quality in terms of both correctness and diversity. To remove noisy paraphrase candidates that are incorrect or duplicates, we manually verified the paraphrase candidates with native English speaker human annotators. Following the annota-

	Paraphrasing Score: 5 Query: <i>Two children smiling on top of luggage in parking lot.</i> Paraphrased query: <i>Two kids grinning atop suitcases in a parking lot.</i>
	Paraphrasing Score: 4 Query : <i>A slice of pizza that is on top of a napkin.</i> Paraphrased query: <i>A piece of pizza that is on top of a paper towel.</i>
	Paraphrasing Score: 3 Query: <i>There is a cat laying down on a keyboard.</i> Paraphrased query: <i>A cat is stretched out on a keyboard.</i>
	Paraphrasing Score: 2 Query: <i>Two skiers prepare to make their way past an embankment.</i> Paraphrased query: <i>Two skiers are getting ready to go around a big hill.</i>
	Paraphrasing Score: 1 Query: <i>A person skating on some pieces of wood.</i> Paraphrased query: <i>A person skating on a rink made of ice.</i>

Figure 2. **Paraphrased samples by GPT-3.** We show five sample images, their original queries, and the corresponding paraphrases generated by GPT-3. From top to bottom, we show the human-provided semantic similarity scores. A semantic similarity score of 5 indicates that the paraphrase has an identical meaning to the original query.

tion protocol in [2, 10], the original and paraphrase candidate sentences are graded with a similarity score between 0 and 5. A sentence pair that are paraphrases and identical in meaning has a similarity score of 5 (i.e. perfect paraphrase). After removal of duplicate and paraphrase pairs with similarity score less than 5, there are 4155 captions with at least one perfect paraphrase. For each of the captions, one perfect paraphrase was randomly chosen for our benchmark.

Evaluating the Rank Similarity of Paraphrased Queries.

In addition to evaluating zero-shot retrieval/classification accuracy of a trained vision-language model, we seek to measure the rank similarity of the top-returned visual search results for a language query and its paraphrase. Typically, it is important for a search engine to show a user the most important search results first. Therefore, an ideal rank similarity metric should satisfy two conditions: (1) it should compare the top- k retrieval list for two queries, and (2) it should weight more heavily the top-most retrieved results. While Spearman’s and Kendall’s [32] rank correlation coefficients measure the rank similarity for a pair of full retrieval lists, they are unable to handle the aforementioned conditions (retrieval list truncation, top-retrieval weighting). We instead measure (top- k average overlap and top- k Jaccard

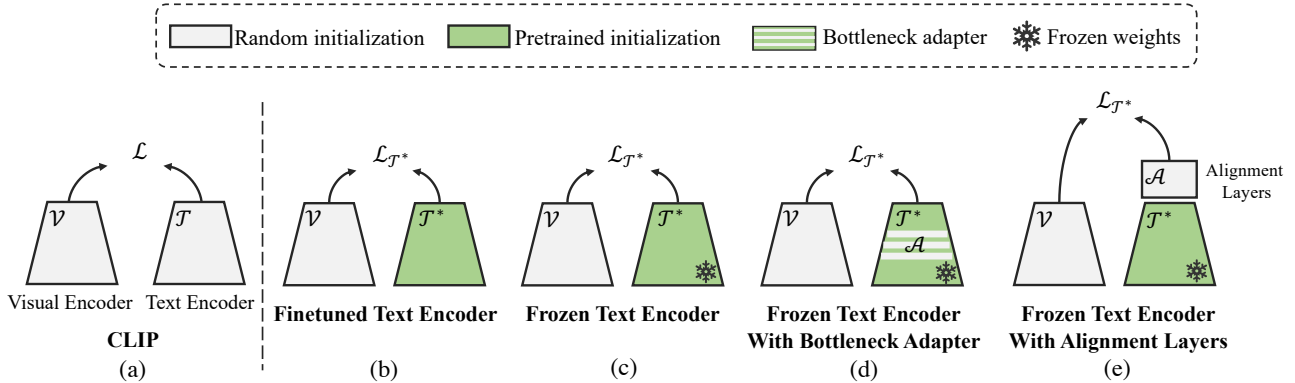


Figure 3. **Adapting pre-trained language models for paraphrased retrieval.** We explore different strategies to adapt pre-trained language models for paraphrased retrieval. (a) illustrates the CLIP baseline, which trains a dual encoder that optimizes the InfoNCE Loss (\mathcal{L}). For CLIP, both the visual encoder (\mathcal{V}) and text encoder (\mathcal{T}) are trained with random initialization. (b-e) illustrate the adaptation strategies that we study – all leveraging a pre-trained language encoder \mathcal{T}^* while training the visual encoder from scratch. This set of adaptation approaches optimize a loss $\mathcal{L}_{\mathcal{T}^*}$. (b) finetunes the text encoder weights, (c) freezes the text encoder weights, (d) inserts bottleneck adapter [6, 28] layers \mathcal{A} to the text encoder, and (e) appends alignment layers, \mathcal{A} , atop of the text encoder.

similarity), which are widely used for computing the similarity of top- k retrieval lists of web search engines [7, 25] and recommendation systems [43].

Let L_q and L_p be rank-ordered retrieval lists for a query q and paraphrase p . The **top- k average overlap** (AO@ k) [22] between the two rank-ordered retrieval lists L_q, L_p is the weighted sum of truncated-list intersections,

$$\text{AO}@k(L_q, L_p) = \frac{1}{k} \sum_{d=1}^k \frac{|L_q^d \cap L_p^d|}{d} \in [0, 1], \quad (1)$$

where $L_q^d = L_q[1 : d]$, $L_p^d = L_p[1 : d]$ are truncated lists at depth d and $|L_q^d \cap L_p^d|$ denotes the cardinality of the set intersection of the truncated lists. $\text{AO}@k = 1$ implies that L_q^k, L_p^k are identical, while $\text{AO}@k = 0$ implies that there is no overlap between L_q^k, L_p^k . Note that $\text{AO}@k$ is top-weighted as the early retrievals appear in more of the summation terms than the lower retrievals.

We also measure the **top- k Jaccard similarity** (JS@ k) [30], computed as the ratio of the top- k intersection over union,

$$\text{JS}@k(L_q, L_p) = \frac{|L_q^k \cap L_p^k|}{|L_q^k \cup L_p^k|} \in [0, 1]. \quad (2)$$

JS@ k is minimized when L_q^k, L_p^k are disjoint and maximized when L_q^k, L_p^k contain the same retrievals (although they may not necessarily be in the same order). Note that the Jaccard similarity can handle retrieval list truncation, but it does not weight top retrievals. In general, higher AO@ k and JS@ k indicate that two top- k lists are more similar.

4. Adapting a Pretrained Language Model for Paraphrased Retrieval

Given a dataset \mathcal{D} of image-text pairs, prior work has trained vision \mathcal{V} and language \mathcal{T} dual encoders from scratch using a contrastive InfoNCE loss \mathcal{L} [44],

$$\min_{\mathcal{V}, \mathcal{T}} \mathcal{L}(\mathcal{V}, \mathcal{T}; \mathcal{D}). \quad (3)$$

In this work, we employ the **CLIP** model [47] (illustrated in Figure 3(a)) as baseline.

As we will show in the experiments, the CLIP model often returns very different retrievals for paraphrased queries. Our hypothesis is that CLIP’s learned text encoder does not perform as well on downstream language tasks as state-of-the-art pretrained language models [18, 26, 50]. To validate our hypothesis, we aim to train a dual-encoder model starting from a pretrained language model instead of training the language tower from scratch (random initialization).

In this section, we describe several strategies for learning a dual-encoder model starting from a pretrained language model \mathcal{T}^* . Let $\mathcal{L}_{\mathcal{T}^*}$ be an InfoNCE loss guided by the pretrained language model \mathcal{T}^* . We seek to optimize loss $\mathcal{L}_{\mathcal{T}^*}$ jointly over the vision encoder \mathcal{V} and a set of auxiliary variables \mathcal{A} in the language tower,

$$\min_{\mathcal{V}, \mathcal{A}} \mathcal{L}_{\mathcal{T}^*}(\mathcal{V}, \mathcal{A}; \mathcal{D}). \quad (4)$$

Figure 3(b-e) illustrate the different strategies that we consider in our study, which we describe next.

Finetuned Text Encoder. This strategy sets the auxiliary variables to be the text encoder $\mathcal{A} \leftarrow \mathcal{T}$ and finetunes starting from the pretrained language model \mathcal{T}^* . As we will

show in the experiments, this setting is not optimal for paraphrase retrieval, which is likely due to catastrophic forgetting during training [33, 51].

Frozen Text Encoder. One strategy to avoid catastrophic forgetting in the language tower is to freeze the language encoder to the pretrained model $\mathcal{T} \leftarrow \mathcal{T}^*$ and only optimize the vision encoder \mathcal{V} , *i.e.*, we do not optimize any auxiliary variables ($\mathcal{A} \leftarrow \emptyset$). While this strategy trivially avoids catastrophic forgetting for downstream language tasks, as shown in prior work [64], it significantly degrades the downstream zero-shot text-image retrieval and image classification accuracy. Note that this result also holds when projecting the language feature to the joint vision-language embedding space using a linear or multilayer perceptron projection head.

Frozen Text Encoder with Bottleneck Adapter. To overcome the issues with the previous strategies, we seek to increase the adaptation ability of the language encoder while preserving the knowledge from the pretrained language model. To achieve this goal, we freeze the language encoder to the pretrained transformer model $\mathcal{T} \leftarrow \mathcal{T}^*$ and insert a set of trainable bottleneck adapter modules [6, 28] \mathcal{A} in each transformer layer. In this work, we employed bottleneck adapters with a reduction factor of 2 at all layers of the frozen pretrained text transformer.

Frozen Text Encoder with Alignment Layers. As an alternate adaptation strategy, we also try appending additional transformer layers \mathcal{A} after the frozen text transformer $\mathcal{T} \leftarrow \mathcal{T}^*$. Since these additional layers are used to align the text embedding with the image embedding, we refer to them as *alignment layers* in this work. In our practice, the alignment layers are set to have the same structure as the frozen text transformer layers with randomly initialized weights.

5. Experiments

The experiment section consists of three parts. Firstly, we ablate various adaptation alternatives and method designs (Section 5.1). Secondly, we compare our approach to a query expansion baseline in Section 5.2. Lastly, in Section 5.3, we assess the scalability of our final model.

Evaluation tasks, datasets, and criteria.

Paraphrased retrieval. We evaluate paraphrase ranking similarity on the benchmark proposed in Section 3. The benchmark includes two testing subsets: COCO Paraphrase (COCO-P) and COCO Paraphrase Extended (COCO-PE). We report top-10 Average Overlap (AO@10) and top-10 Jaccard Similarity (JS@10).

Classification and retrieval. We evaluate zero-shot classification on ImageNet 1K (IN-1K) [16] and report Top-1 accuracy. We also evaluate zero-shot image retrieval on the Flickr30k [45] and COCO Captions (COCO) [38] datasets. For retrieval, we report the average Recall at 5 (R@5).

Text semantic similarity. We evaluate the zero-shot capa-

bilities of the text encoder on the Semantic Textual Similarity Benchmark (STS-B) [10] without finetuning. This dataset is widely used to measure the language understanding ability of language models. We adopt the Spearman [32] and Pearson rank correlation coefficients for measuring the STS performance.

Implementation Details. We train our models on the Conceptual Captions 12M (CC12M) [11] for ablation study in Sections 5.1 and 5.2. Our visual encoder (\mathcal{V}) is randomly initialized and employs a ViT-B/32 architecture [20] as a backbone. The text encoder (\mathcal{T}) adopts the DistilRoBERTa-base [55] backbone. This text transformer model has 6 layers, 12 heads, a 768 dimensional embedding space, and ~ 82 M parameters in total (comparable to ~ 65 M parameters for the text encoder of CLIP (ViT-B/32) [48]). We initialize the text encoder leveraging weights provided by the sentence-transformer [50], which were pretrained on the OpenWebText Corpus [24] and then finetuned on 1B sentences. We use a linear layer and a 2-layer MLP to project the visual and language embedding to the same multi-modal latent space, respectively. We closely follow the training procedure of CLIP [48] and trained all our models in automatic mixed precision with an AdamW optimizer [39], and a cosine annealing learning rate schedule. Our models were trained for 32 epochs including 10000 steps of linear warm-up. Additional hyper-parameters are reported in the supplementary material.

5.1. Ablation Study: Adaptation on CC12M

Adaptation strategies. We investigate different adaptation strategies for training a dual-encoder model starting from a pretrained text encoder. We evaluate the CLIP baseline [48] (Figure 3(a)) and the four different adaptation strategies introduced in Section 4:

\mathcal{T} *finetuned* (Figure 3(b)). Finetunes a pre-trained text encoder without additional trainable layers.

\mathcal{T} *frozen* (Figure 3(c)). Freezes a pre-trained text encoder without additional trainable layers.

\mathcal{T} *frozen + bottleneck* (Figure 3(d)). Inserts bottleneck adapters [6, 28] to a pre-trained (and frozen) text encoder.

\mathcal{T} *frozen + alignment* (Figure 3(e)). Appends $m = 6$ alignment layers to a pre-trained (and frozen) text encoder.

We present the most important comparisons in Table 1 and include the full ablation results in the supplementary material (Tables B.2 & B.3).

(a) Effect on paraphrased retrieval (Table 1a).

We observe that approaches with a frozen pretrained text encoder always achieve significantly higher paraphrase ranking similarity. They outperform significantly the CLIP baseline. On the contrary, with the same pre-trained initialization, the paraphrase ranking similarity of \mathcal{T} *finetuned* drops to the level of CLIP. We attribute that result to catastrophic forgetting of the rich text pre-training, and hypothesize that

	COCO-P		COCO-PE			IN-1K	Flickr30k	COCO	STS-B		
	AO@10	JS@10	AO@10	JS@10		Acc.	R@5	R@5	Pearson	Spearman	
CLIP	50.9	42.5	33.8	26.4	CLIP	29.0	67.2	35.8	CLIP	71.8	71.6
\mathcal{T} finetuned	51.9	44.9	34.0	26.7	\mathcal{T} finetuned	28.5	67.7	34.9	\mathcal{T} finetuned	72.4	72.9
\mathcal{T} frozen	65.6	56.9	52.0	42.9	\mathcal{T} frozen	18.7	52.9	25.8	\mathcal{T} frozen	82.1	83.3
\mathcal{T} frozen + bottleneck	65.5	57.0	52.7	43.1	\mathcal{T} frozen + bottleneck	18.8	53.3	25.5	\mathcal{T} frozen + bottleneck	82.2	83.4
\mathcal{T} frozen + alignment	68.3	60.2	55.2	46.1	\mathcal{T} frozen + alignment	29.0	69.7	35.8	\mathcal{T} frozen + alignment	79.0	79.6

(a) **Paraphrased retrieval.** All adaptation approaches boost ranking similarity (AO@10 and JS@10). Adapting with alignment layers offers the largest gain.

(b) **Classification and retrieval.** Adapting with alignment layers yields higher or comparable zero-shot classification (top-1 accuracy) and image retrieval (R@5) performance to the CLIP baseline.

(c) **Text semantic similarity.** All adaptation approaches boost the semantic similarity performance. Adapting with alignment layers achieves competitive performance.

	number of alignment layers					initialization of \mathcal{V}	
	0	2	4	6	8	random	ImageNet
retrieval (COCO)	25.8	33.1	35.4	35.8	36.4	35.8	45.9
paraphrased retrieval (COCO-P)	52.0	55.4	55.5	55.2	55.3	55.2	55.1
text semantic similarity	82.1	79.9	79.8	79.0	78.3	79.0	78.9

(d) **Effect of number of alignment layers.** We ablate the number of layers of \mathcal{T} frozen + alignment, our best adaptation. Appending layers improves image retrieval but saturates around 6 layers, has a minor impact in paraphrased retrieval (AO@10) and text semantic similarity (Pearson).

(e) **Effect of initialization of \mathcal{V} .** We vary the initialization of the visual encoder between random and ImageNet weights. ImageNet init. boosts the retrieval performance but does not improve paraphrased retrieval.

Table 1. **Adaptation on CC12M ablation studies.** We trained the CLIP baseline and our adaptation variants on the CC12M dataset. We conduct all experiments in a zero-shot fashion. See the text for a discussion of the results.

	COCO	COCO-P
CLIP (w/o QE)	35.8	50.9
CLIP + QE w/ WordNet	34.8	52.4
CLIP + QE w/ Parrot	36.7	53.9
Ours (w/o QE)	35.8	68.3

Table 2. **Comparison to Query Expansion (QE).** We evaluate two query expansion techniques on image retrieval (R@5) and paraphrased retrieval (AO@10). We compare to our method (\mathcal{T} frozen + alignment) and observe that our solution achieves significantly higher paraphrased retrieval (COCO-P). All models are trained on CC12M.

such forgetting emerges from fine-tuning on millions of noisy image-text pairs.

(b) Effect on classification and retrieval (Table 1b).

First, we observe that the frozen text encoder has significantly worse retrieval/classification accuracy than CLIP, which is consistent with the observation reported in LiT [64]. The introduction of the bottleneck adapters failed to make up the accuracy gap. Meanwhile, the approaches of finetuning and introducing alignment layers are shown to achieve comparable, and sometimes even better, zero-shot accuracy than the baseline CLIP method. Note that our finetuning result is consistent with the result reported in LiT [64].

(c) Effect on text semantic similarity (Table 1c).

We employ the text encoder of each adaptation strategy to the semantic textual similarity task on the STS-B dataset.

\mathcal{T} frozen achieves high scores, which is expected given that the language model is trained on a text corpora. Surprisingly, the \mathcal{T} frozen + bottleneck language encoder slightly outperforms the \mathcal{T} frozen language model. While \mathcal{T} frozen + alignment has slightly lower scores, it is significantly better than CLIP and \mathcal{T} finetuned.

(d) Effect of the number of alignment layers (Table 1d).

Through ablations (a-c), we found that the strategy of appending alignment layers to a frozen pre-trained text encoder (\mathcal{T} frozen + alignment) achieves the best balance between retrieval accuracy, paraphrased ranking similarity, and text semantic similarity performance. Therefore, in this analysis we study the effect of the number of alignment layers of the aforementioned model. We observe that increasing the number of layers is beneficial for all tasks, with performance saturating after 6 layers.

(e) Effect of visual encoder initialization (Table 1e).

We observe that initializing the visual encoder (\mathcal{V}) with ImageNet greatly improves the retrieval performance (R@5 on COCO) compared to random initialization. The performance on paraphrased retrieval and text semantic similarity remains relatively unchanged after varying the visual encoder initialization.

5.2. Comparison to Query Expansion

Query Expansion (QE) is a popular technique to reduce the effect of synonyms on text queries [4, 9]. Accordingly, we evaluate QE on our paraphrased image retrieval benchmark. We consider two different QE approaches: QE via WordNet [41] and QE via automatic paraphrasing. The for-

model	data	paraphrased retrieval				classification and retrieval				text semantic similarity	
		paraphrased text-image retrieval				classification		image retrieval		text semantic similarity	
		COCO-P		COCO-PE		IN-1K	VTAB+	Flickr30k	COCO	STS-B	
		AO@10	JS@10	AO@10	JS@10	Acc.		R@5		Pearson	Spearman
CLIP [48]	WIT-400M	67.0	58.1	52.8	42.6	63.3	45.5	83.4	56.0	65.6	69.5
OpenCLIP [13]	LAION-400M	68.1	59.5	51.5	42.5	62.9	45.8	85.5	60.9	75.2	75.7
Ours	LAION-400M	73.7	66.1	60.2	50.8	60.5	46.6	84.0	60.0	80.3	81.0

Table 3. **Large Scale Adaptation on LAION-400M.** We compare our adaptation method (\mathcal{T} frozen + alignment) with baselines, all trained at large scale, and evaluated on multiple zero-shot tasks: paraphrased retrieval, classification and retrieval, and text semantic similarity. All models use the ViT-B/32 architecture as the visual backbone and are trained for 32 epochs on the specified dataset. For VTAB+, we report the average top-1 accuracy over 35 tasks following the setup in [57].

mer expands a sentence query by replacing one of its non-stop words with a synonym provided by WordNet. The latter expands sentence queries by generating automatic paraphrases leveraging the T5-based [49] Parrot paraphrasing model [14]. Given a query sentence q^{txt} and K expanded queries $\{q_i^{\text{txt}}\}_{i=1}^K$, our goal is to obtain a QE-expanded text feature \mathbf{z}^{new} , and then use it to compute the cosine similarity against the visual features in the retrieval set. This new text feature is formed by averaging the text feature of the original query and the K expanded queries,

$$\mathbf{z}^{\text{new}} = \frac{1}{K+1} \left(\mathcal{T}(q^{\text{txt}}) + \sum_{i=1}^K \mathcal{T}(q_i^{\text{txt}}) \right). \quad (5)$$

The results of combining query expansion and the CLIP *baseline* model in Section 5.1 are listed in Table 2. Both QE techniques slightly improve ranking similarity in the paraphrased retrieval task. However, their effectiveness is limited compared to our adaptation approach. In addition, we observe a drop in image retrieval accuracy for QE w/ WordNet. We suspect this drop is due to the use of incorrect synonyms resulting from imperfect word sense disambiguation. In light of these results, we argue that QE (alone) is not sufficient for addressing the limitations of CLIP’s dual encoder for the paraphrase retrieval task.

5.3. Large-scale Adaptation on LAION-400M

In this section, we study the performance of our best model, Frozen Text Encoder with Alignment Layers (\mathcal{T} frozen + alignment), trained on a large-scale dataset. We train our model using the LAION-400M dataset [56], which contains about 413M image-text pairs. Our model’s visual backbone is randomly initialized. We compare our method with CLIP (ViT-B/32) [48] model and OpenCLIP (ViT-B/32) [29]. Note that CLIP employs a private dataset, while OpenCLIP leverages the same training dataset as our adaptation approach. The training total batch size is set as 32760. Our model is trained for 32 epochs using 40 NVIDIA A100 80GB GPUs in one week. For CLIP and OpenCLIP, we use their publicly available model weights.

	COCO	COCO-TP
CLIP [48]	361.8	308.1 (-14.8%)
OpenCLIP [13]	381.6	329.3 (-13.7%)
Ours	371.6	335.3 (-9.8%)

Table 4. Evaluations of Robustness to text perturbations on COCO-TP [46]. RSUM (*i.e.*, $\sum_{k \in \{1,5,10\}} \text{IR R}@k + \text{TR R}@k$) is employed as evaluation metrics.

Table 3 summarizes the results on three different tasks. In this setting, we added the VTAB+ [57, 63] benchmark as an additional comparison for classification. This benchmark includes 35 different datasets, and has become widely adopted to evaluate the zero-shot capabilities of large scale pre-trained models. Consistently with the results in Section 5.1, our model improves upon the CLIP and OpenCLIP baselines on the paraphrased retrieval task. As an example, our model achieves 60.2% AO@10 on COCO-PE, which represents a +7.4% gain with respect to the most competitive baseline (CLIP). For classification and retrieval, our model achieves competitive/comparable performance for most of the datasets, and improves +0.8% on VTAB+, arguably one of the most challenging benchmarks. Finally, we also observe that the text encoder of our adapted model is much more appealing for text semantic similarity. Our model improves over the most competitive baseline (OpenCLIP) by 5.1% on this task.

In Figure 4, we show qualitative results of our approach and compare against CLIP. Notice how, in general, the top retrievals for our approach has more images that are in common between the query and paraphrased query (outlined in green) than the CLIP baseline. Moreover, our approach handles phrase synonyms (first, third examples) and full sentence paraphrases (second example). The bottom result shows a failure case where our approach underperforms CLIP, likely due to forgetting during training.

In addition to the evaluation discussed above, we compared our model with CLIP and OpenCLIP on COCO-



Figure 4. **Qualitative results** for CLIP [48] (left) and our approach (right). We outline images in green that appear in the top-10 retrievals for both the query and paraphrased query. The full top-10 retrievals can be found in the supplementary material (Figures B.1 & B.2). Please see the text for a discussion of the results.

TP [46], a benchmark of the robustness of vision-language models to different types of text perturbations. Higher robustness of our model to text perturbations is observed in Table 4 and can be considered as a beneficial side effect of our adaption strategy.

6. Conclusion

We have demonstrated an effective strategy for training a dual-encoder vision-language model by adapting from a

pretrained language model. Our strategy yields significantly improved paraphrased retrieval on our newly collected paraphrased text-image dataset. Our dual encoder’s text tower also improves on the downstream text semantic similarity task. Moreover, our strategy maintains downstream zero-shot classification and retrieval accuracy. Our work opens up the possibility of an improved natural language search interface and a tighter coupling between strong language models and learned visual representations.

References

- [1] Quora question pairs. <https://www.kaggle.com/c/quora-question-pairs>. 3
- [2] Eneko Agirre, Daniel Cer, Mona Diab, Aitor Gonzalez-Agirre, and Weiwei Guo. *SEM 2013 shared task: Semantic textual similarity. In *Second Joint Conference on Lexical and Computational Semantics (*SEM), Volume 1: Proceedings of the Main Conference and the Shared Task: Semantic Textual Similarity*, 2013. 3
- [3] Jean-Baptiste Alayrac, Jeff Donahue, Pauline Luc, Antoine Miech, Iain Barr, Yana Hasson, Karel Lenc, Arthur Mensch, Katherine Millican, Malcolm Reynolds, et al. Flamingo: a visual language model for few-shot learning. 2022. 2
- [4] Hiteshwar Kumar Azad and Akshay Deepak. Query expansion techniques for information retrieval: a survey. *Information Processing & Management (IPM)*, 56(5):1698–1735, 2019. 2, 6
- [5] Ricardo A. Baeza-Yates and Berthier A. Ribeiro-Neto. *Modern Information Retrieval*. ACM Press / Addison-Wesley, 1999. 2
- [6] Ankur Bapna and Orhan Firat. Simple, scalable adaptation for neural machine translation. In *EMNLP*, 2019. 4, 5
- [7] Judit Bar-Ilan, Mazlita Mat-Hassan, and Mark Levene. Methods for comparing rankings of search engine results. *Computer networks*, 50(10):1448–1463, 2006. 4
- [8] Tom Brown, Benjamin Mann, Nick Ryder, Melanie Subbiah, Jared D Kaplan, Prafulla Dhariwal, Arvind Neelakantan, Pranav Shyam, Girish Sastry, Amanda Askell, et al. Language models are few-shot learners. In *NeurIPS*, 2020. 2, 3
- [9] Claudio Carpineto and Giovanni Romano. A survey of automatic query expansion in information retrieval. *ACM Computing Surveys (CSUR)*, 44(1):1–50, 2012. 2, 6
- [10] Daniel Cer, Mona Diab, Eneko Agirre, Iñigo Lopez-Gazpio, and Lucia Specia. SemEval-2017 task 1: Semantic textual similarity multilingual and crosslingual focused evaluation. In *Proceedings of the 11th International Workshop on Semantic Evaluation (SemEval-2017)*, 2017. 2, 3, 5
- [11] Soravit Changpinyo, Piyush Sharma, Nan Ding, and Radu Soricut. Conceptual 12m: Pushing web-scale image-text pre-training to recognize long-tail visual concepts. In *CVPR*, 2021. 5
- [12] Yen-Chun Chen, Linjie Li, Licheng Yu, Ahmed El Kholy, Faisal Ahmed, Zhe Gan, Yu Cheng, and Jingjing Liu. Uniter: Universal image-text representation learning. In *ECCV*, 2020. 2
- [13] Mehdi Cherti, Romain Beaumont, Ross Wightman, Mitchell Wortsman, Gabriel Ilharco, Cade Gordon, Christoph Schuhmann, Ludwig Schmidt, and Jenia Jitsev. Reproducible scaling laws for contrastive language-image learning. *arXiv preprint arXiv:2212.07143*, 2022. 7, 15, 16
- [14] Prithiviraj Damodaran. Parrot: Paraphrase generation for nlu., 2021. 7
- [15] Scott Deerwester, Susan T Dumais, George W Furnas, Thomas K Landauer, and Richard Harshman. Indexing by latent semantic analysis. *Journal of the American society for information science*, 41(6):391–407, 1990. 2
- [16] Jia Deng, Wei Dong, Richard Socher, Li-Jia Li, Kai Li, and Li Fei-Fei. Imagenet: A large-scale hierarchical image database. In *CVPR*, 2009. 5
- [17] Karan Desai, Gaurav Kaul, Zubin Aysola, and Justin Johnson. Redcaps: web-curated image-text data created by the people, for the people. In *NeurIPS Datasets and Benchmarks*, 2021. 2
- [18] Jacob Devlin, Ming-Wei Chang, Kenton Lee, and Kristina Toutanova. BERT: Pre-training of deep bidirectional transformers for language understanding. In *NAACL-HLT*, 2019. 4
- [19] Bill Dolan and Chris Brockett. Automatically constructing a corpus of sentential paraphrases. In *Third International Workshop on Paraphrasing*, 2005. 2, 3
- [20] Alexey Dosovitskiy, Lucas Beyer, Alexander Kolesnikov, Dirk Weissenborn, Xiaohua Zhai, Thomas Unterthiner, Mostafa Dehghani, Matthias Minderer, Georg Heigold, Sylvain Gelly, Jakob Uszkoreit, and Neil Houlsby. An image is worth 16x16 words: Transformers for image recognition at scale. In *ICLR*, 2021. 5
- [21] Rahim Entezari, Mitchell Wortsman, Olga Saukh, M. Moein Shariatnia, Hanie Sedghi, and Ludwig Schmidt. The role of pre-training data in transfer learning. *arXiv preprint arXiv:2302.13602*, 2023. 2
- [22] Ronald Fagin, Ravi Kumar, and Dakshinamurthi Sivakumar. Comparing top k lists. *SIAM Journal on discrete mathematics*, 17(1):134–160, 2003. 4
- [23] Kevin R. Gee. Using Latent Semantic Indexing to Filter Spam. In *Proceedings of the 18th Symposium on Applied Computing*, pages 460–464. ACM, 2003. 2
- [24] Aaron Gokaslan and Vanya Cohen. Openwebtext corpus. <http://Skylion007.github.io/OpenWebTextCorpus>, 2019. 5
- [25] Aniko Hannak, Piotr Sapiezynski, Arash Molavi Kakhki, Balachander Krishnamurthy, David Lazer, Alan Mislove, and Christo Wilson. Measuring personalization of web search. In *WWW*, 2013. 4
- [26] Pengcheng He, Xiaodong Liu, Jianfeng Gao, and Weizhu Chen. Deberta: Decoding-enhanced bert with disentangled attention. In *ICLR*, 2021. 4
- [27] Chaitra Hegde and Shrikumar Patil. Unsupervised paraphrase generation using pre-trained language models. *arXiv preprint arXiv:2006.05477*, 2020. 3
- [28] Neil Houlsby, Andrei Giurgiu, Stanislaw Jastrzebski, Bruna Morrone, Quentin De Laroussilhe, Andrea Gesmundo, Mona Attariyan, and Sylvain Gelly. Parameter-efficient transfer learning for nlp. In *ICML*, 2019. 4, 5
- [29] Gabriel Ilharco, Mitchell Wortsman, Ross Wightman, Cade Gordon, Nicholas Carlini, Rohan Taori, Achal Dave, Vaishaal Shankar, Hongseok Namkoong, John Miller, Hananeh Hajishirzi, Ali Farhadi, and Ludwig Schmidt. Openclip, 2021. 7
- [30] Paul Jaccard. The distribution of the flora in the alpine zone. *New phytologist*, 11(2):37–50, 1912. 4
- [31] Chao Jia, Yinfei Yang, Ye Xia, Yi-Ting Chen, Zarana Parekh, Hieu Pham, Quoc Le, Yun-Hsuan Sung, Zhen Li, and Tom Duerig. Scaling up visual and vision-language representation learning with noisy text supervision. In *ICML*, 2021. 2

- [32] Maurice George Kendall. *Rank correlation methods*. Griffin, 1948. 3, 5
- [33] James Kirkpatrick, Razvan Pascanu, Neil Rabinowitz, Joel Veness, Guillaume Desjardins, Andrei A. Rusu, Kieran Milan, John Quan, Tiago Ramalho, Agnieszka Grabska-Barwinska, Demis Hassabis, Claudia Clopath, Dharshan Kumaran, and Raia Hadsell. Overcoming catastrophic forgetting in neural networks. *Proceedings of the National Academy of Sciences (PNAS)*, 114(13):3521–3526, 2017. 5
- [34] Thomas K Landauer, Peter W Foltz, and Darrell Laham. An introduction to latent semantic analysis. *Discourse processes*, 25(2-3):259–284, 1998. 2
- [35] Junnan Li, Ramprasaath Selvaraju, Akhilesh Gotmare, Shafiq Joty, Caiming Xiong, and Steven Chu Hong Hoi. Align before fuse: Vision and language representation learning with momentum distillation. In *NeurIPS*, 2021. 2
- [36] Junnan Li, Dongxu Li, Caiming Xiong, and Steven Hoi. Blip: Bootstrapping language-image pre-training for unified vision-language understanding and generation. In *ICML*, 2022.
- [37] Junnan Li, Dongxu Li, Silvio Savarese, and Steven Hoi. Blip-2: Bootstrapping language-image pre-training with frozen image encoders and large language models. *arXiv preprint arXiv:2301.12597*, 2023. 2
- [38] Tsung-Yi Lin, Michael Maire, Serge Belongie, James Hays, Pietro Perona, Deva Ramanan, Piotr Dollár, and C Lawrence Zitnick. Microsoft coco: Common objects in context. In *ECCV*, 2014. 3, 5
- [39] Ilya Loshchilov and Frank Hutter. Decoupled weight decay regularization. In *ICLR*, 2019. 5
- [40] Christopher D. Manning, Prabhakar Raghavan, and Hinrich Schütze. *Introduction to Information Retrieval*. Cambridge University Press, 2008. 2
- [41] George A Miller. Wordnet: a lexical database for english. *Communications of the ACM*, 38(11):39–41, 1995. 2, 6
- [42] George A Miller, Richard Beckwith, Christiane Fellbaum, Derek Gross, and Katherine J Miller. Introduction to wordnet: An on-line lexical database. *International journal of lexicography*, 3(4):235–244, 1990. 2
- [43] Sejoon Oh, Berk Ustun, Julian McAuley, and Srijan Kumar. Rank list sensitivity of recommender systems to interaction perturbations. In *CIKM*, 2022. 4
- [44] Aaron van den Oord, Yazhe Li, and Oriol Vinyals. Representation learning with contrastive predictive coding. *arXiv preprint arXiv:1807.03748*, 2018. 4
- [45] Bryan A Plummer, Liwei Wang, Chris M Cervantes, Juan C Caicedo, Julia Hockenmaier, and Svetlana Lazebnik. Flickr30k entities: Collecting region-to-phrase correspondences for richer image-to-sentence models. In *ICCV*, 2015. 5
- [46] Jielin Qiu, Yi Zhu, Xingjian Zhen, Zhiqiang Tang, Ding Zhao, Bo Li, and Mu Li. Benchmarking robustness under distribution shift of multimodal image-text models. In *NeurIPS 2022 Workshop on Distribution Shifts (DistShifts)*, 2022. 2, 7, 8, 15
- [47] Alec Radford, Jeff Wu, Rewon Child, David Luan, Dario Amodei, and Ilya Sutskever. Language models are unsupervised multitask learners. 2019. 3, 4
- [48] Alec Radford, Jong Wook Kim, Chris Hallacy, Aditya Ramesh, Gabriel Goh, Sandhini Agarwal, Girish Sastry, Amanda Askell, Pamela Mishkin, Jack Clark, Gretchen Krueger, and Ilya Sutskever. Learning transferable visual models from natural language supervision. In *ICML*. PMLR, 2021. 1, 2, 5, 7, 8, 15, 16, 17, 18
- [49] Colin Raffel, Noam Shazeer, Adam Roberts, Katherine Lee, Sharan Narang, Michael Matena, Yanqi Zhou, Wei Li, and Peter J. Liu. Exploring the limits of transfer learning with a unified text-to-text transformer. *Journal of Machine Learning Research (JMLR)*, 21(140):1–67, 2020. 7
- [50] Nils Reimers and Iryna Gurevych. Sentence-BERT: Sentence embeddings using Siamese BERT-networks. In *EMNLP*, 2019. 4, 5
- [51] Anthony Robins. Catastrophic forgetting, rehearsal and pseudorehearsal. *Connection Science*, 7(2):123–146, 1995. 5
- [52] J. J. Rocchio. Relevance feedback in information retrieval. In *The Smart retrieval system - experiments in automatic document processing*, pages 313–323. Englewood Cliffs, NJ: Prentice-Hall, 1971. 2
- [53] Ian Ruthven and Mounia Lalmas. A survey on the use of relevance feedback for information access systems. *The Knowledge Engineering Review*, 18(2):95–145, 2003. 2
- [54] Chitwan Saharia, William Chan, Saurabh Saxena, Lala Li, Jay Whang, Emily Denton, Seyed Kamyar Seyed Ghasemipour, Burcu Karagol Ayan, S. Sara Mahdavi, Rapha Gontijo Lopes, Tim Salimans, Jonathan Ho, David J Fleet, and Mohammad Norouzi. Photorealistic text-to-image diffusion models with deep language understanding. In *NeurIPS*, 2022. 2
- [55] Victor Sanh, Lysandre Debut, Julien Chaumond, and Thomas Wolf. Distilbert, a distilled version of bert: smaller, faster, cheaper and lighter. *arXiv preprint arXiv:1910.01108*, 2019. 5
- [56] Christoph Schuhmann, Richard Vencu, Romain Beaumont, Robert Kaczmarczyk, Clayton Mullis, Aarush Katta, Theo Coombes, Jenia Jitsev, and Aran Komatsuzaki. Laion-400m: Open dataset of clip-filtered 400 million image-text pairs. *arXiv preprint arXiv:2111.02114*, 2021. 7
- [57] Christoph Schuhmann, Romain Beaumont, Richard Vencu, Cade W Gordon, Ross Wightman, Mehdi Cherti, Theo Coombes, Aarush Katta, Clayton Mullis, Mitchell Wortsman, Patrick Schramowski, Srivatsa R Kundurthy, Katherine Crowson, Ludwig Schmidt, Robert Kaczmarczyk, and Jenia Jitsev. LAION-5b: An open large-scale dataset for training next generation image-text models. In *Thirty-sixth Conference on Neural Information Processing Systems Datasets and Benchmarks Track*, 2022. 7
- [58] Amanpreet Singh, Ronghang Hu, Vedanuj Goswami, Guillaume Couairon, Wojciech Galuba, Marcus Rohrbach, and Douwe Kiela. Flava: A foundational language and vision alignment model. In *CVPR*, 2022. 2
- [59] Jan Philip Wahle, Terry Ruas, Frederic Kirstein, and Bela Gipp. How large language models are transforming machine-paraphrased plagiarism. In *EMNLP*, 2022. 3
- [60] Sam Witteveen and Martin Andrews. Paraphrasing with

- large language models. *arXiv preprint arXiv:1911.09661*, 2019. 3
- [61] Antoine Yang, Antoine Miech, Josef Sivic, Ivan Laptev, and Cordelia Schmid. Zero-shot video question answering via frozen bidirectional language models. In *NeurIPS*, 2022. 2
- [62] Lewei Yao, Runhui Huang, Lu Hou, Guansong Lu, Minzhe Niu, Hang Xu, Xiaodan Liang, Zhenguo Li, Xin Jiang, and Chunjing Xu. FILIP: Fine-grained interactive language-image pre-training. In *ICLR*, 2022. 2
- [63] Xiaohua Zhai, Joan Puigcerver, Alexander Kolesnikov, Pierre Ruysen, Carlos Riquelme, Mario Lucic, Josip Djolonga, Andre Susano Pinto, Maxim Neumann, Alexey Dosovitskiy, Lucas Beyer, Olivier Bachem, Michael Tschannen, Marcin Michalski, Olivier Bousquet, Sylvain Gelly, and Neil Houlsby. A large-scale study of representation learning with the visual task adaptation benchmark. *arXiv preprint arXiv:1910.04867*, 2019. 7
- [64] Xiaohua Zhai, Xiao Wang, Basil Mustafa, Andreas Steiner, Daniel Keysers, Alexander Kolesnikov, and Lucas Beyer. Lit: Zero-shot transfer with locked-image text tuning. In *CVPR*, 2022. 2, 5, 6
- [65] Pengchuan Zhang, Xiujun Li, Xiaowei Hu, Jianwei Yang, Lei Zhang, Lijuan Wang, Yejin Choi, and Jianfeng Gao. Vinvl: Revisiting visual representations in vision-language models. In *CVPR*, 2021. 2
- [66] Jianing Zhou and Suma Bhat. Paraphrase generation: A survey of the state of the art. In *EMNLP*, 2021. 3

Adapting Dual-encoder Vision-language Models for Paraphrased Retrieval Supplementary Material

A. Paraphrased Text-Image Retrieval Dataset

A.1. Samples.

We present 10 samples from our paraphrased text-image retrieval dataset in Figure A.1.

Image	Caption
	Original Query: A <i>little</i> cat <i>looking at itself</i> in a mirror. Paraphrased Query: A <i>small</i> cat <i>gazing at its reflection</i> in a mirror.
	Original Query: A person <i>dressed as a giraffe</i> carrying a <i>bullhorn</i> . Paraphrased Query: A person <i>wearing a giraffe costume</i> and carrying a <i>megaphone</i> .
	Original Query: a sandwich that <i>has</i> something green and red <i>in it</i> Paraphrased Query: A sandwich that <i>contains</i> something green and red.
	Original Query: A bowl of some broccoli <i>that is</i> chopped. Paraphrased Query: A bowl of some <i>chopped</i> broccoli.
	Original Query: A <i>large</i> red and white bus on <i>a city street</i> . Paraphrased Query: A <i>big</i> red and white bus on <i>an urban road</i> .
	Original Query: <i>Some kids</i> standing up playing <i>wii with each other</i> Paraphrased Query: <i>A group of children</i> are playing <i>the Wii console together while standing up</i> .
	Original Query: A dog <i>on a leash</i> <i>trying</i> to ride a skateboard. Paraphrased Query: A dog <i>restrained</i> by a leash <i>attempting</i> to ride a skateboard.
	Original Query: some <i>planes</i> on an <i>air port</i> run way Paraphrased Query: Some <i>aircraft are positioned</i> on a runway <i>at an airport</i> .
	Original Query: A man <i>kneeling down</i> in front of a <i>refrigerator</i> . Paraphrased Query: A man <i>on his knees</i> in front of a <i>fridge</i> .
	Original Query: A man <i>riding skis</i> down a <i>snow covered</i> slope. Paraphrased Query: A man <i>skiing</i> down a <i>snowy</i> slope.

Figure A.1. Paraphrased text-image retrieval dataset samples.

A.2. Hyperparameters.

We list the GPT-3 hyperparameters used for automatic paraphrase collection in Table A.1.

Hyperparameter	Value
prompt	<i>“Paraphrase the following sentence, using as many synonyms as possible: {Input}”</i>
engine	text-davinci-002
temperature	0.9
max tokens	32

Table A.1. Hyperparameters for paraphrase collection by GPT-3.

B. Experiment

B.1. Hyperparameters.

We list the training hyperparameters used for all our models in Table B.1.

Hyperparameter	Value
batch size	4000 (CC12M), 32760 (LAION-400M)
training epochs	32
warm-up iterations	10000
learning rate	0.001
AdamW weight decay	0.1
AdamW β_1	0.9
AdamW β_2	0.999 (RN50), 0.98 (ViT-B/32)
AdamW ϵ	10^{-8} (RN50), 10^{-6} (ViT-B/32)

Table B.1. Hyperparameters for our training experiments.

B.2. Adaptation on CC12M.

The full ablation on the choice of image encoders (network architecture and initialization strategy) and adaptation methods is presented in Tables B.2 and B.3.

B.3. Large-scale Adaptation on LAION-400M.

The performances for zero-shot classification and image retrieval of different models are compared in Table B.4. The zero-shot classification accuracies of different models on 35 VTAB+ datasets are compared in Table B.6. We present the top-10 retrieved images for the qualitative examples of Figure 4 in Figures B.1 and B.2.

B.4. Query Expansion (QE) details.

For our evaluation of QE in Section 5.2, we set the number of expanded queries as $K = 3$.

			Classification	Text Retrieval				Image Retrieval			
\mathcal{V}	Init. \mathcal{V}	Method	ImageNet Acc.	Flickr30k R@1	Flickr30k R@5	COCO R@1	COCO R@5	Flickr30k R@1	Flickr30k R@5	COCO R@1	COCO R@5
RN50	Random	CLIP	33.6	47.5	75.8	19.4	42.0	43.0	71.8	18.9	41.5
		\mathcal{T} finetuned	33.2	50.1	76.3	20.8	44.8	44.2	73.0	19.4	34.2
		\mathcal{T} frozen	20.1	31.1	60.9	12.4	31.8	28.1	55.4	11.9	27.6
		\mathcal{T} frozen + bottleneck	21.9	32.7	62.4	13.0	32.2	29.6	58.1	12.3	29.5
		\mathcal{T} frozen + alignment	33.7	54.7	80.5	23.9	47.7	49.7	76.5	20.5	44.5
	ImageNet	CLIP	36.9	48.5	78.3	22.5	46.3	48.2	73.1	22.4	45.8
		\mathcal{T} finetuned	37.3	51.6	79.5	24.2	47.3	48.8	75.7	22.7	46.2
		\mathcal{T} frozen	30.6	44.8	73.2	21.9	46.2	40.8	67.7	20.3	43.3
		\mathcal{T} frozen + bottleneck	33.2	52.1	78.6	25.0	49.4	46.8	75.0	22.4	46.8
		\mathcal{T} frozen + alignment	37.8	54.5	81.1	26.7	51.3	50.6	76.9	24.0	48.0
ViT-B/32	Random	CLIP	29.0	43.2	68.1	16.6	37.5	41.0	67.2	16.0	35.8
		\mathcal{T} finetuned	28.5	44.4	70.2	17.8	38.1	40.9	67.7	15.5	34.9
		\mathcal{T} frozen	18.7	27.3	57.6	11.7	29.4	26.1	52.9	10.2	25.8
		\mathcal{T} frozen + bottleneck	18.8	30.2	57.8	11.4	28.7	26.2	53.3	9.2	25.5
		\mathcal{T} frozen + alignment	29.0	45.6	72.2	18.2	40.1	41.2	69.7	15.9	35.8
	ImageNet	CLIP	36.8	52.3	77.8	20.8	45.5	49.7	75.1	20.0	42.0
		\mathcal{T} finetuned	30.2	42.9	71.6	16.5	38.6	39.2	66.9	16.0	38.6
		\mathcal{T} frozen	36.3	53.2	78.1	21.0	45.1	49.9	77.3	19.8	40.8
		\mathcal{T} frozen + bottleneck	30.7	42.3	70.9	17.2	38.8	39.2	67.3	15.1	36.3
		\mathcal{T} frozen + alignment	37.5	54.6	80.7	21.8	46.4	51.9	80.0	20.6	45.9

Table B.2. Performance of different models on zero-shot classification and image/text retrieval. All models are trained for 32 epochs on the CC12M dataset.

			paraphrased text-image retrieval				semantic text similarity	
\mathcal{V}	Init. \mathcal{V}	Method	COCO-P		COCO-PE		STS-B	
			AO@10	JS@10	AO@10	JS@10	Pearson/%	Spearman/%
RN50	Random	CLIP	51.7	43.4	34.6	27.2	68.3	68.2
		\mathcal{T} finetuned	53.0	44.9	35.1	28.1	71.0	69.9
		\mathcal{T} frozen	68.6	60.6	54.2	45.4	82.8	83.9
		\mathcal{T} frozen + bottleneck	67.4	60.3	53.9	43.9	73.6	75.0
		\mathcal{T} frozen + alignment	69.0	60.9	55.3	46.3	76.7	78.8
	ImageNet	CLIP	53.7	44.9	35.7	28.1	68.4	68.5
		\mathcal{T} finetuned	55.3	45.1	36.4	28.3	69.2	69.3
		\mathcal{T} frozen	69.2	61.4	55.5	46.1	81.6	83.1
		\mathcal{T} frozen + bottleneck	68.6	60.7	54.5	45.3	73.6	75.8
		\mathcal{T} frozen + alignment	69.8	61.2	55.3	46.0	76.7	78.7
ViT-B/32	Random	CLIP	50.9	42.5	33.8	26.4	71.8	71.6
		\mathcal{T} finetuned	51.9	44.9	34.0	26.7	72.4	72.9
		\mathcal{T} frozen	65.6	56.9	52.0	42.9	82.1	83.3
		\mathcal{T} frozen + bottleneck	65.5	57.0	52.7	43.1	82.2	83.4
		\mathcal{T} frozen + alignment	68.3	60.2	55.2	46.1	79.0	79.6
	ImageNet	CLIP	53.2	44.6	35.5	28.0	70.0	69.7
		\mathcal{T} finetuned	53.9	44.5	35.6	28.4	72.1	72.9
		\mathcal{T} frozen	66.6	58.6	53.4	43.9	81.1	82.9
		\mathcal{T} frozen + bottleneck	66.8	58.1	52.8	43.4	81.7	83.2
		\mathcal{T} frozen + alignment	68.8	60.7	55.1	45.9	78.9	80.0

Table B.3. Performance of different models on paraphrased text-image retrieval and semantic text similarity. All models are trained for 32 epochs on the CC12M dataset.

model	data	classification			image retrieval					
		IN-1K Top-1 Acc.	IN-1K Top-5 Acc.	VTAB+ Top-1 Acc.	R@1	Flickr30k R@5	Flickr30k R@10	R@1	COCO R@5	COCO R@10
CLIP[48]	WIT-400M	63.3	88.8	45.5	58.8	83.4	89.8	30.4	56.0	66.9
OpenCLIP [13]	LAION-400M	62.9	87.7	45.8	61.7	85.5	90.9	35.3	60.9	71.6
Ours	LAION-400M	60.5	86.0	46.6	59.9	84.0	90.7	33.9	60.0	70.6

Table B.4. Large scale adaptation on LAION-400M. All models use the ViT-B/32 architecture as the visual backbone and are trained for 32 epochs on the specified dataset.

	Clean	Character-level						Word-level					Sentence-level					Avg.
		K	OCR	CI	CR	CS	CD	SR	WI	WS	WD	IP	P	A	F	C	BT	
CLIP	361.8	235.0 ↓35.1%	294.4 ↓18.6%	253.3 ↓30.0%	236.7 ↓34.6%	247.1 ↓31.7%	249.6 ↓31.0%	313.3 ↓13.4%	330.1 ↓8.8%	319.2 ↓11.8%	332.4 ↓8.1%	344.2 ↓4.9%	348.7 ↓3.6%	359.6 ↓0.6%	357.9 ↓1.1%	357.2 ↓1.3%	350.9 ↓3.0%	308.1 ↓14.8%
OpenCLIP	381.8	249.5 ↓34.6%	315.1 ↓17.5%	269.2 ↓29.5%	251.8 ↓34.0%	265.1 ↓30.6%	265.4 ↓30.5%	331.4 ↓13.2%	357.5 ↓6.4%	355.6 ↓6.9%	358.4 ↓6.1%	370.1 ↓3.1%	370.7 ↓2.9%	381.5 ↓0.1%	378.7 ↓0.8%	377.6 ↓1.1%	371.6 ↓2.7%	329.3 ↓13.7%
Ours	371.6	277.1 ↓25.4%	327.2 ↓11.9%	310.6 ↓16.4%	278.4 ↓25.1%	293.9 ↓20.9%	290.1 ↓21.9%	334.3 ↓10.0%	353.6 ↓4.8%	355.9 ↓4.2%	352.4 ↓5.1%	361.6 ↓2.7%	362.8 ↓2.3%	370.6 ↓0.3%	368.4 ↓0.9%	368.6 ↓0.8%	358.6 ↓3.5%	335.3 ↓9.8%

Table B.5. Evaluation of robustness to three different levels of text perturbation on COCO-TP [46]. The types of perturbation are: a) **Character-level**: keyboard (K), OCR, character insert (CI), character replace (CR), character swap (CS), character delete (CD); b) **Word-level**: synonym replacement (SR), word insertion (WI), word swap (WS), word deletion (WD), and insert punctuation (IP); c) **Sentence-level**: formal (F), casual (C), passive (P), active (A), back translation (BT).

data	CLIP [48] WIT-400M	OpenCLIP [13] LAION-400M	Ours LAION-400M
ImageNet	63.3	62.9	60.5
ImageNet-v2	55.9	55.1	52.5
ImageNet-R	69.2	73.5	71.0
ImageNet-Sketch	42.3	49.4	46.6
ObjectNet	44.2	43.9	42.8
ImageNet-A	31.4	21.7	21.1
CIFAR-10	89.8	90.8	92.4
CIFAR-100	64.3	70.3	71.8
MNIST	48.7	37.6	61.6
Flowers102	66.4	68.0	56.5
Cars	59.7	79.3	78.3
SVHN	13.5	27.7	38.3
FER2013	41.3	43.0	42.9
RenderedSST2	58.6	52.4	56.7
Pets	87.3	86.9	83.2
Caltech-101	81.6	83.2	82.9
VOC2007-C1	76.4	75.8	75.5
SUN397	62.3	67.0	66.0
FGVC Aircraft	19.6	16.6	12.0
Country211	17.2	14.8	13.9
DTD	44.3	54.6	56.0
GTSRB	32.6	42.0	44.1
STL10	97.1	95.6	96.5
Retino	44.8	25.2	63.2
EuroSAT	50.5	51.5	42.2
RESISC45	53.7	54.6	52.7
PCAM	62.3	55.8	61.4
CLEVR Counts	23.2	16.2	16.3
CLEVR Dist	23.4	23.9	20.0
DSPRITES Orient	2.5	1.9	2.2
DSPRITES Pos	3.4	3.0	3.2
SmallNORB Elv	12.8	4.5	11.3
SmallNORB Azim	6.1	9.9	4.9
DMLAB	19.3	17.3	17.3
KITTI Dist	27.4	29.1	17.6
VTAB+ (Avg.)	45.5	45.8	46.6

Table B.6. Zero-shot classification accuracies on VTAB+ 35 tasks. All models use the ViT-B/32 architecture as the visual backbone and are trained for 32 epochs on the specified dataset.

	q_1 : "A road sign that indicates route <i>sixty six</i> ." (top row)									
	p_1 : "A road sign that indicates Route <i>66</i> ." (bottom row)									
CLIP [48]										
Ours										
	q_2 : "An open refrigerator filled with lots of food." (top row)									
	p_2 : "A fridge that is open and has a lot of food inside." (bottom row)									
CLIP [48]										
Ours										
	q_3 : "A cat <i>sitting on the back of a sofa</i> looking out a window." (top row)									
	p_3 : "A cat <i>perched atop a sofa</i> gazing out a window." (bottom row)									
CLIP [48]										
Ours										

Figure B.1. Some examples where our model increases the top-10 ranking similarity in paraphrased text-to-image retrieval.

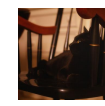
	q_4 : "A toy horse <i>sits atop</i> a red wooden chair." (top row)									
	p_4 : "A toy horse <i>is perched on top of</i> a red wooden chair." (bottom row)									
CLIP [48]										
										
Ours										
										

Figure B.2. An example where our model fails to increase the top-10 ranking similarity in paraphrased text-to-image retrieval.